Engineering Science and Technology, an International Journal 18 (2015) 463–474

HOSTED BY

ELSEVIER

Contents lists available at ScienceDirect

Engineering Science and Technology, an International Journal

journal homepage: http://www.elsevier.com/locate/jestch

Full length article

Adhesive friction at the contact between rough surfaces using n-point asperity model

Ajay K. Waghmare, Prasanta Sahoo*

Department of Mechanical Engineering, Jadavpur University, Kolkata 700 032, India

ARTICLE INFO

Article history:
Received 19 December 2014
Received in revised form
9 March 2015
Accepted 9 March 2015
Available online 25 April 2015

Keywords:
Adhesive friction
n-point asperity
Elastic–plastic contact
Rough surface
Adhesion index
Plasticity index

ABSTRACT

The paper describes a theoretical study of adhesive friction at elastic–plastic contact of rough surfaces based on n-point asperity model. Well defined adhesion index and plasticity index are used to study the prospective situations arising out of variation in load, material properties, and surface roughness. Results are obtained for the behavior of friction force, applied load, and coefficient of friction for different combinations of adhesion index, plasticity index and mean separation of surfaces. The results obtained are in line with earlier models. It is observed that the tensile load required in maintaining a separation increases with increase in adhesion effect and extent of plastic deformation. Also coefficient of friction increases with adhesion effect.

1. Introduction

Adhesion is one of the contributing factors to friction effect, particularly in micro and nano-scale contact of rough surfaces. It is well established that macro scale systems are more influenced by inertia effects while micro scale systems are more influenced by surface effects. Thus study of adhesional friction has become important particularly in a micro electro-mechanical system (MEMS) that miniaturizes contacting elements. Bowden and Tabor [1] proposed their adhesive friction theory by introducing the concept of real area of contact where adhesive friction is described as a tangential force required to shear off the adhesive bonds formed at the tip of contacting asperities due to local plastic deformation of asperities. The theory is well established and supported by great many experimental results. Skinner and Gane [2] have described experiments to measure friction at micro-contacts. Their experimental work was carried out in a vacuum with a typically single asperity contact condition under extremely light loads or even negative loads. The influence of a tangential force on adhesive contact has been studied experimentally by Savkoor and Briggs [3]. To describe adhesive component of friction, Johnson [4] considered both interfacial sliding and tearing of intermetallic micro junctions and named it as 'tangential interaction'. Pollock [5] described in detail how surface forces may influence a wide range of friction processes. Etsion and Amit [6] observed a dramatic increase in the static friction coefficient as the normal load was reduced to its lower level and the behavior is attributed to the role played by adhesion forces which are more pronounced at small loads and smooth surfaces. Israelachvili et al. [7] have also presented results of their experiments using surface force apparatus technique that correlates systematically adhesion and both static and kinetic friction forces. Roy Chowdhury and Ghosh [8] investigated adhesive contact and friction using well known JKR model [9] of adhesion and showed that at low loads and high elastic adhesion indices the coefficient of adhesional friction depends on material parameters. A multi-asperity contact model, which included adhesion using the DMT model [10], was presented by Maugis [11]. Although the friction force was not determined, it was speculated that the increase in contact force due to adhesion would result in increased friction. The concept of fracture mechanics is used to explain the relationship between the adhesion and friction at the contact of solid surfaces in the work of Johnson [12]. Researchers have used scale independent fractal approach [13] as well as scale dependent approach [14] to describe adhesive friction between rough solids. Studies incorporating asperity interaction [15] in elastic–plastic adhesive friction contact have shown that the

* Corresponding author.
E-mail addresses: psjume@gmail.com, psahoo@mech.jdvu.ac.in (P. Sahoo).
Peer review under responsibility of Karabuk University.

http://dx.doi.org/10.1016/j.jestch.2015.03.006

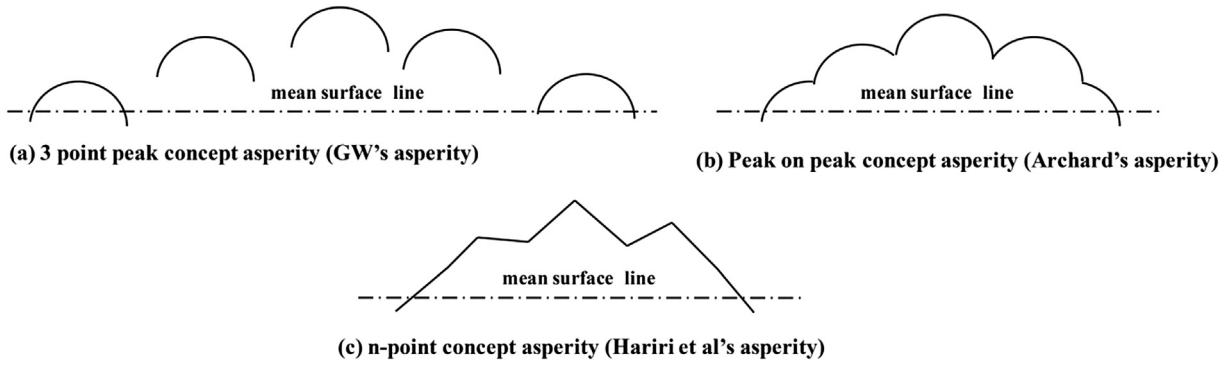

Fig. 1. Illustrating different asperity concepts.

coefficient of friction depends strongly on the applied load for no-interaction case while it becomes insensitive to the load for interaction consideration. Kogut and Etsion [16] developed a static friction model for elastic–plastic contacting rough surfaces in which they incorporated the results of accurate finite element analyses for the elastic–plastic contact, adhesion and sliding inception of a single asperity. They have shown that there is a strong effect of external force and nominal contact area on the static friction coefficient in contrast to classical laws of friction.

Greenwood and Williamson [17] in their pioneering statistical model of contact between rough surfaces used hemi-spherically tipped asperities of identical radius of curvature with heights following a Gaussian distribution. Asperity height ordinates are decided with three point peak concept (a summit higher than its neighboring two on the same profile). Most of the models found in the literature are mainly based on this three point peak model. In spite of the wide acceptance of this model, Greenwood and Wu [18] brought their original idea of three-point peak under question and called it inadequate because it gives false idea of both the radius of curvature of asperities and the number of asperities. They suggested considering asperities as protuberances on protuberances on protuberances which was originally proposed by Archard [19]. Hariri et al. [20] presented a multi-point asperity model called as n-point asperity model in which each asperity is assumed to be composed of (n) neighboring points with (n−2) middle points above a certain level (h). Hariri et al. [20] used Archard's peak on peak on peak concept for definition of their asperity but with some modification. They used straight line profiles to connect the peak ordinates and named their asperity as n-point asperity where n is the indicator of number of peak ordinates of which the asperity is composed of. Fig. 1 illustrates the basic difference in definition of these asperities. As can be seen in Fig. 2 (a) and (b) in n-point asperity model, asperity curvature as well as height changes with the progression of contact. Also with decrease in separation, the previous asperity gets merged into a new asperity with higher number of n-points. Thus as compared to conventional Greenwood and Williamson model [17], the n-point asperity model represents the rough surfaces in more realistic form as it considers the variation in form of asperities in vertical direction (asperity height direction) as well as horizontal direction (asperity spacing direction). Based on this new n-point asperity model, the elastic/plastic normal contact problems both non-adhesive [21] and adhesive contact [22] have been considered earlier. However, to the best of the authors' knowledge, no study is available on analysis of adhesive friction of contacting surfaces that involves n-point asperity model. The present study attempts to analyze adhesive frictional contact using this n-point asperity model framework.

2. Statistical definition of n-point asperity

As the n-point asperity model developed by Hariri et al. [20] is the foundation of the present work, it is necessary to outline in brief the salient features of this model in order to set a scene for the formulation of the present problem. Figs. 1 and 2 describe the physical form of n-point asperity. But in statistical terms, the n-point asperity becomes an entity containing n number of random variables. From probabilistic point of view, existence of an n-point asperity at a particular level h means occurrence of a set of n neighboring ordinates with the condition that middle (n−2) height ordinates exist above the level and two end ordinates exist below the level. Considering these n consecutive points as height ordinates $z_1,\ldots,z_n$, the occurrence of an n-point asperity is defined by an event $S=\{z_1<h,z_2,\ldots z_{n-1}>h,z_n<h\}$. Probability of existence of this event S can be given as (a separate list of notations is given)

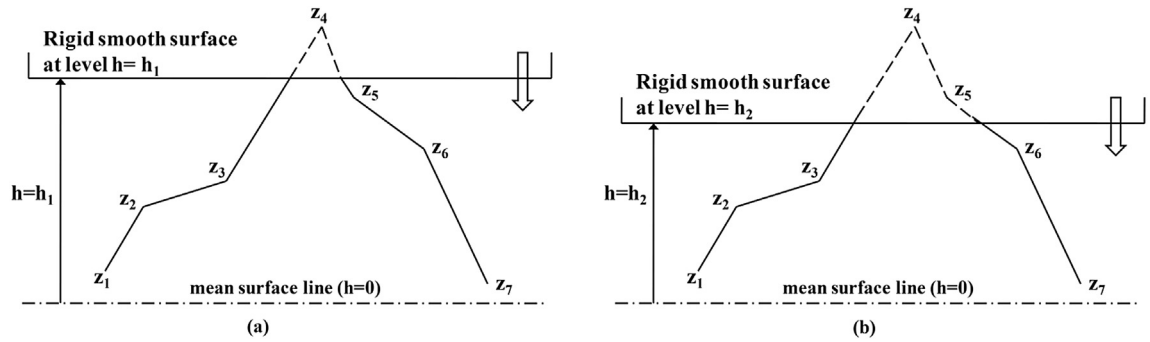

Fig. 2. Progression of contact and emergence of new asperity.

$$N_n = \int_{z_1=-\infty}^{h} \int_{z_2=h}^{\infty} \ldots \int_{z_i=h}^{\infty} \ldots \int_{z_{n-1}=h}^{\infty} \int_{z_n=-\infty}^{h} f_{z_1,\ldots z_n}(z_1,\ldots z_n)\,dz_n dz_{n-1}\ldots dz_i\ldots dz_2 dz_1 \quad (1)$$

where $f_{z1\ldots\ldots zn}(z_1,\ldots,z_n)$ is the joint pdf for event S in which each ordinate follows Gaussian distribution. The resultant joint pdf will also follow Gaussian distribution and it is given as

$$f_{z_1\ldots z_n}(z_1,\ldots\ldots,z_n) = \frac{e^{-z_1^2/2}}{(2\pi)^{n/2}(1-\rho^2)^{(n-1)/2}} \prod_{i=n-1}^{1} e^{-\left[(z_{i+1}-\rho z_i)^2/2(1-\rho^2)\right]} \quad (2)$$

If we consider total M number of sample points on the surface then the number of points in contact for all asperities composed of n number of ordinates will be M_n which is obtained as

$$M_n = M \times N_n \quad (3)$$

If these M sample points are obtained from a square grid formed by $(m \times m)$ perpendicular lines on a plane having separation between two consecutive lines as Δx, then $M = m^2$ and total nominal contact area of this grid is

$$A_0 = \Delta x^2 M \quad (4)$$

In order to facilitate the analysis, Hariri et al. [20] replaced the n-point asperity by an equivalent parabolic asperity as shown in Fig. 3. The equivalent parabolic asperity is defined in terms of two parameters viz. height (z_0^*) and curvature coefficient (c_n) the details of which are omitted here for brevity and available in Hariri et al. [20].

3. Analysis of adhesive friction

Analysis of adhesive frictional contact has earlier been carried out [8] assuming conventional three point asperities over the surface. These three point asperities are assumed to be hemispherical (at least near the tip point) with identical radius and varying heights. The present study considers n-point asperities where both the height and radius vary. It is well established that adhesion phenomenon is mainly observed on very smooth surfaces i.e. for surfaces having micro and nano scale size asperities. Thus the analysis of adhesive friction using n-point asperities taken up here correspond to profiles having micro scale size roughness or lower. The distribution and size of larger scale asperities are important in analyzing mechanical interactions but do not affect the present analysis. Deformation of larger scale asperities leads to bulk deformation and is ignored. In following two sub-sections loading analysis for elastic–plastic deformation and frictional load formulations involving slip and yield phenomenon are considered in n-point asperity model framework.

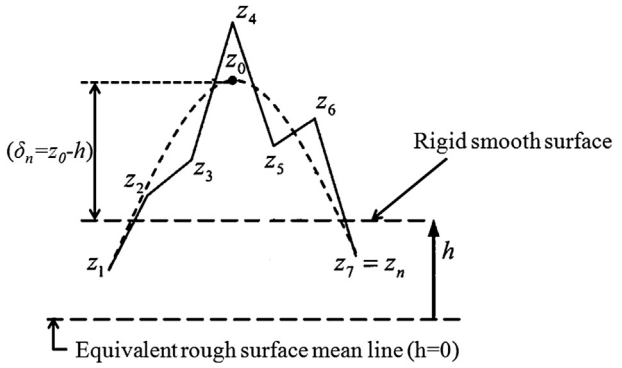

Fig. 3. n-point asperity and equivalent parabolic asperity.

3.1. Elastic-plastic loading analysis

Based on Greenwood and Williamson's postulate it is considered that the average size of a micro-contact is almost constant and is independent of load. Thus in loading analysis it is considered that surfaces will always have some asperities elastically loaded and some fully plastically loaded. Following the analysis of JKR model [9] of contact between a smooth sphere and a flat in presence of adhesion, the load on an elastically deformed asperity is given by

$$\Delta P_{(e)_n} = \frac{K a_{(e)_n}^3}{R_n} - \left(6\pi\gamma K a_{(e)_n}^3\right)^{\frac{1}{2}} \quad (5)$$

Where $\Delta P_{(e)_n}$ is the load supported by single n-point asperity having specific 'n' value in elastic domain, $K = 4/3E$, E is the composite elastic modulus given by $E = [(1-\upsilon_1^2)/E_1 + (1-\upsilon_2^2)/E_2]^{-1}$, E_1, E_2, υ_1 and υ_2 being the elastic moduli and Poisson's ratios of the contacting surfaces respectively, $a_{(e)_n}$ is contact radius of an n-point asperity in elastic mode of deformation, R_n is the equivalent radius of an n-point asperity, γ is the work of adhesion. Following Hertz contact law, the contact radius of an n-point asperity in elastic mode of deformation is given by $a_{(e)_n} = (R_n\delta_n)^{1/2}$ where interference of an n-point asperity is $\delta_n = z_0 - h$. Here z_0 is the height of n-point asperity, h is the mean separation.

Following the approach of Roy Chowdhury and Pollock [23], the load on a plastically deformed n-point asperity in presence of adhesion is given by

$$\Delta P_{(p)_n} = \pi a_{(p)_n}^2 H - 2\pi R_n \gamma \quad (6)$$

where $\Delta P_{(p)_n}$ is the load supported by single n-point asperity having specific 'n' value in plastic domain and H the hardness. Here contact radius of an n-point asperity in plastic mode of deformation is given by $a_{(p)_n} = (2R_n\delta_n)^{1/2}$. The equivalent radius of n-point asperity is given by $R_n = [(n-1)\Delta x/2]^2/c_n\sigma$ with sampling length, $\Delta x = \beta^*(-In\rho)$. β^* is the correlation length and ρ is the correlation coefficient.

It has already been mentioned that in n-point asperity model, the complex n-point asperity profile is converted into equivalent parabolic asperity profile. The quantitative parameters (equivalent height z_0 and radius R_n) of this best fit profile which is shown by dotted line in Fig. 3 are obtained by equating the areas under the profiles. In order to obtain a generalized solution, the applied load in equations (5) and (6) are normalized with the load unit term A_0H; A_0 being the total nominal contact area of rough surface. In this normalization process, two non dimensional indices viz. adhesion index [22] $\phi = \gamma\beta^*/E\sigma^2$ and plasticity index [21] $\psi = H\beta^*/E\sigma$ are used. For a single n-point asperity, expressions for non-dimensional load for an elastically deformed asperity and plastically deformed asperity are given by

$$\Delta P^*_{(e)_n} = \frac{(n-1)}{(-\ln \rho)} \left\{ \frac{2\delta^{*3/2}_n}{3\psi c^{1/2}_n} - \frac{1.77(n-1)^{1/2}(-\ln \rho)^{1/2}\phi^{1/2}\delta^{*3/4}_n}{\psi c^{3/4}_n} \right\} \tag{7}$$

$$\Delta P^*_{(p)_n} = \frac{\pi(n-1)^2}{2}\left(\frac{\delta^*_n}{c_n} - \frac{\phi}{c_n\psi}\right) \tag{8}$$

It is well established fact that the plastic deformation of an asperity commences when the mean contact pressure on the asperity reaches or exceeds its hardness value. Thus the plasticity condition is written as

$$\frac{\Delta P_{(e)_n}}{\pi a^2_{(e)_n}} \geq H \tag{9}$$

which leads to

$$\delta^{3/4}_{(1)_n} - \left(\frac{2.36H}{E^*}\right) R^{1/2}_n \delta^{1/4}_{(1)_n} - 3.76\left(\frac{\gamma}{E^*}\right)^{1/2} R^{1/4}_n \geq 0 \tag{10}$$

In above equations δ_n and $\delta_{(1)_n}$ are actual and apparent interference of an asperity. Following Ref. [22], the normalized critical values $\delta^*_{(c)_n}$, $\delta^*_{(c_1)_n}$ and $c_{(1)_n}$ marking transition from elastic to plastic state can be determined by solving a set of three equations as given below.

$$\delta^{*3/4}_{(c_1)_n} - 1.18(n-1)(-\ln \rho)\psi \frac{\delta^{*1/4}_{(c_1)_n}}{c^{1/2}_{(1)_n}} - 2.66\{(n-1)(-\ln \rho)\}^{1/2}\phi^{1/2}\frac{1}{c^{3/4}_{(1)_n}} = 0 \tag{11}$$

$$\delta^*_{(c)_n} = \delta^*_{(c_1)_n} - 1.77\phi^{1/2}\{(n-1)(-\ln \rho)\}^{1/2}\frac{\delta^{*1/4}_{(c_1)_n}}{c^{1/4}_{(1)_n}} \tag{12}$$

$$c_{(1)_n} = 2\delta^*_{(c_1)_n} \tag{13}$$

Now to model the behavior of rough surface, we need to obtain an ensemble of asperities by statistical approach. Also from the study of Greenwood and Tripp [24] and O'Callaghan and Cameron [25] it can be seen that the situation of contact between two rough surfaces can be simplified as a contact between a rigid smooth surface and an equivalent rough surface and the same consideration is used in the present study. So considering now the contact between a rigid smooth surface and a rough deformable surface (as shown in Fig. 4) with Gaussian joint pdf of n neighboring ordinates which gives M_n number of n-point asperities in contact (*viz.* $M_{(e)_n}$ number of asperities in elastic and $M_{(p)_n}$ number of asperities in plastic contact), the applied load for this group of n-point asperities

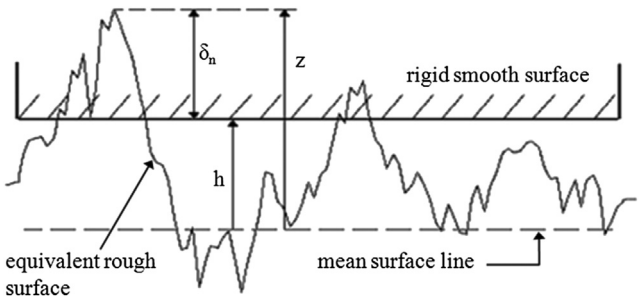

Fig. 4. Contact of equivalent rough surface and rigid smooth surface.

is calculated by taking product of number of asperities in contact and the expected value of applied load.

$$P^*_{(e)_n} = M_{(e)_n} E\left[\Delta P^*_{(e)_n}\right] \quad \text{for } \delta^*_{(0)_n} \leq \delta^*_n \leq \delta^*_{(c_1)_n} \tag{14}$$

$$P^*_{(p)_n} = M_{(p)_n} E\left[\Delta P^*_{(p)_n}\right] \quad \text{for } \delta^*_{(c)_n} \leq \delta^*_n \leq \infty \tag{15}$$

$$P^*_n = P^*_{(e)_n} + P^*_{(p)_n} \tag{16}$$

Total applied load for all n-point asperities is the summation of all P^*_n calculated for all n values and it is,

$$P^* = \sum_{n=3}^{\infty} P^*_n \tag{17}$$

In equations (14) and (15), Δ values are for a single n-point asperity for a specified n value and are given by equations (7) and (8).E[.] is the expectation operator which is the symbolic representation of mathematical procedure followed to calculate average or mean value of a random variable in defined range of variation and with defined pattern of distribution of the random variable in that range [20]. The detailed procedure for calculation of loads on all elastically and plastically deformed asperities has been provided in Appendix A.1 and A.2 respectively.

3.2. Frictional force analysis

The classical theory of adhesive friction does not consider the effect of surface forces as for large-scale asperities adhesion is insignificant. On the other hand, for small scale asperities deformation and friction at very smooth and clean surfaces are strongly affected by surface forces. It may be noted here that even atomically smooth surfaces contain small scale roughness features. Friction at these surfaces depends on surface properties including surface energy, small scale roughness and micro-mechanical material properties. Both surface energy and mechanical shear failure play a role in friction at such contacts and we only consider the important one. The frictional force for such asperities on the surface is the force offering resistance to tangential movement and plastically deformed asperities offer negligible resistance [8]. The initially elastically deformed asperities contribute to friction force until yielding occurs under the combined action of normal load and tangential force. The other group of asperities which remain elastic even under the combined effect of normal and shear stresses will undergo slip. Thus the frictional resistance for deformation up to plastic limit is composed of two parts: a) Frictional resistance before tangential slip ($\Delta T_{(slip)_n}$) and b) Frictional resistance before yielding ($\Delta T_{(yield)_n}$). The frictional resistance for the asperities where slip occurs before yielding can be obtained using Savkoor and Briggs [3] energy balance approach, and the same when formulated for an n-point asperity by incorporating adhesion and plasticity indices and normalized with respect to load term A_0H yields frictional resistance offered by an n-point asperity before slip in non dimensional form. It is given by

$$\Delta T^*_{(slip)_n} = 2.5\left(\frac{1-\nu}{2-\nu}\right)^{\frac{1}{2}}\left(\frac{\phi}{\psi}\right)\left\{\frac{(n-1)^3}{(-\ln \rho)\phi}\left(\frac{\delta^*_n}{c_n}\right)^{\frac{3}{2}} - 1.77\frac{(n-1)^4}{c^2_n}\right\}^{\frac{1}{2}} \tag{18}$$

Beyond slip point there exist some asperities which are still elastic under combined effect of tangential and normal stresses and these asperities also contribute to frictional resistance until

yielding takes place. So it becomes necessary to find out plasticity condition at the area of contact on an n-point asperity. The plasticity condition is based on incipient yielding at the surface and is obtained by using von-Mises criterion in conjunction with Hamilton [26] stress field. The plasticity condition in non dimensional form for an n-point asperity then works out as

$$C_1\frac{\delta_n^{*3}}{c_n}+C_2\frac{\delta_n^{*9/4}}{c_n^{5/4}}+C_3\frac{\delta_n^{*2}}{c_n^{2}}+\left(C_4+C_5\Delta T^*_{(slip)_n}c_n\right)\frac{\delta_n^{*3/2}}{c_n^{3/2}}+C_6\Delta T^*_{(slip)_n}\frac{\delta_n^{*3/4}}{c_n^{3/4}}+C_7{\Delta T^*_{(slip)_n}}^2=0 \tag{19}$$

The constants in above equationC_1,C_2, etc. are given below.

$$C_1=\frac{0.034(n-1)^2(1-4\nu+4\nu^2)}{(-\ln\rho)^2\psi^2}$$

$$C_2=-\frac{0.18(n-1)^{5/2}(1-4\nu+4\nu^2)\phi^{1/2}}{(-\ln\rho)^{3/2}\psi^2}$$

$$C_3=-\frac{(n-1)^4}{116.64}$$

$$C_4=\frac{0.024(n-1)^3(1-4\nu+4\nu^2)\phi}{(-\ln\rho)\psi^2}$$

$$C_5=\frac{0.12(n-1)(2-5\nu+2\nu^2)}{(-\ln\rho)\psi}$$

$$C_6=-\frac{0.32(n-1)^{3/2}(2-5\nu+2\nu^2)\phi^{1/2}}{(-\ln\rho)^{1/2}\psi}$$

$$C_7=0.035\left(16-4\nu+7\nu^2\right)$$

Solution of equation (19) gives the apparent critical values of interference ($\delta^*_{(tc_1)_n}$) and curvature coefficient ($c_{(t_1)_n}$) for tangential slip. All n-point asperities having interference $\delta_n^*<\delta^*_{(tc_1)_n}$ will contribute to tangential slip resistance. Thus the non dimensional frictional force due to all such n-point asperities is obtained by evaluating the product of number of n-point asperities in such contact and the expected value of $\Delta T^*_{(slip)_n}$ in the interference range $\delta^*_{(0)_n}$ to$\delta^*_{(tc_1)_n}$.

$$T^*_{(slip)_n}=M_{(slip)_n}E\left[\Delta T^*_{(slip)_n}\right]\quad\text{for interference range}\quad\delta^*_{(0)_n}\le\delta_n^*\le\delta^*_{(tc_1)_n} \tag{20}$$

Asperities in the interference range $\delta^*_{(tc_1)_n}\le\delta_n^*\le\delta^*_{(c_1)_n}$ do not deform plastically and still offer some tangential resistance. The frictional or tangential force contributed by such n-point asperities is obtained by replacing $\Delta T^*_{(slip)_n}$ by $\Delta T^*_{(yield)_n}$ in equation (19) and solving it for$\Delta T^*_{(yield)_n}$. This solution gives two roots for $\Delta T^*_{(yield)_n}$ as given below.

$$\Delta T^*_{(yield)_n}=\frac{-\left(Term\ I\pm(Term\ II)^{1/2}+Term\ III\right)}{Term\ IV} \tag{21}$$

$$Term\ I=C_6\,c_n^{1/4}\delta_n^{*3/4}$$

$$Term\ II=\left(C_6^2c_n^{1/2}\delta_n^{*3/2}+C_5^2c_n\delta_n^{*3}-4C_3C_7\delta_n^{*2}-4C_1C_7c_n\delta_n^{*3}-4C_2C_7c_n^{3/4}\delta_n^{*9/4}-4C_4C_7c_n^{1/2}\delta_n^{*3/2}+2C_5C_6c_n^{3/4}\delta_n^{*9/4}\right)^{\frac{1}{2}}$$

$$Term\ III=C_5c_n^{1/2}\delta_n^{*3/2}$$

$$Term\ IV=2C_7c_n$$

So the non dimensional frictional force before yield for a particular group of n-point asperities is calculated as

$$T^*_{(yield)_n}=M_{(yield)_n}E\left[\Delta T^*_{(yield)_n}\right]\quad\text{for}\quad\delta^*_{(tc_1)_n}\le\delta_n^*\le\delta^*_{(c_1)_n} \tag{22}$$

Total frictional force contributed by a particular group of n-point asperities is

$$T_n^*=T^*_{(slip)_n}+T^*_{(yield)_n} \tag{23}$$

Total frictional force on the whole surface in contact is

$$T^*=\sum_{i=3}^{n}T_n^* \tag{24}$$

The detailed expressions for tangential slip load and yield load are provided in Appendix A.3 and A.4 respectively.

Solution of equation (20) requires the expression for apparent zero interference$\delta^*_{(0)_n}$ in n-point asperity model framework. Roy Chowdhury and Ghosh [8] followed JKR theory [9] for adhesive contact analysis which involves apparent parameters of loading and deformation and to relate these apparent values with actual ones, Johnson relation [27] was used. Following the same approach in the present study, the relationship between actual and apparent values of interference for n-point asperities is given by

$$\delta_n^*=\delta^*_{(1)_n}-1.77\phi^{1/2}\{(n-1)(-\ln\rho)\}^{1/2}\frac{\delta^*_{(1)_n^{1/4}}}{c_n^{1/4}} \tag{25}$$

To get apparent interference corresponding to actual interference of zero, one needs to put $\delta_n^*=0$ and $\delta^*_{(1)_n}=\delta^*_{(0)_n}$ in above equation that yields,

$$0=\delta^*_{(0)_n}-1.77\phi^{1/2}\{(n-1)(-\ln\rho)\}^{1/2}\frac{\delta^*_{(0)_n^{1/4}}}{c_n^{1/4}} \tag{26}$$

Solution of above equation for $\delta^*_{(0)_n}$ gives

$$\delta^*_{(0)_n}=2.14\left\{\frac{\phi^2(n-1)^2(-\ln\rho)^2}{c_n}\right\}^{1/3}. \tag{27}$$

4. Results and discussion

In n-point asperity approach for analyzing the rough surface contact, variation in height, radius and spacing of asperities on rough surface are allowed. So it represents more realistic situation of asperity profile on rough surface as compared to conventional three point asperity approach. But as the number of variable parameters in n-point approach of analysis is increased, the solution of problem becomes more complex. The style of defining the indices like ϕ and ψ which are responsible for creating prospective situations of contact is also different in these two approaches. So it becomes difficult to set a common platform to compare the results obtained by these two approaches. To study adhesive friction behavior of rough surfaces we need to evaluate externally applied

load (P) and tangential or friction load (T) for different contact situations. Non dimensional applied load (P^*) on the rough surface is obtained from equation (17) which in turn is solved numerically by using expressions in equations (28)–(31) given in Appendix. Non dimensional tangential or friction load (T^*) is obtained from equation (24) which in turn is solved numerically by using expressions in equations (32)–(35) given in Appendix. For calculations of tangential load a typical value of Poisson's ratio $\upsilon = 0.3$ is used. Prospective situations of contact are generated by varying the values of adhesion index ($\phi = \gamma\beta^*/E\sigma^2$) and plasticity index($\psi = H\beta^*/E\sigma$). Both these indices are well defined and successfully used in earlier n-point asperity models. The adhesion index (ϕ) [22] combines the adhesion energy per unit contact area (γ), composite elastic modulus of contacting surfaces (E) and surface roughness parameters (β^* and σ). Higher the values of ϕ, higher will be adhesion effect and vice versa. Earlier analysis [22] considered the adhesion index in the range 0.1–0.9. In the present study adhesion index is varied from 0.01(insignificant adhesion effect) to 0.9 (maximum adhesion effect). The plasticity index (ψ) defined by Hariri et al. [21] is function of hardness (H) of the softer of two contacting surfaces, composite elastic modulus of contacting surfaces (E) and surface roughness parameters (β^* and σ) and it gives predominance of nature of contact. According to Hariri et al. [21], contact will be predominantly plastic for $\psi<1.0$, predominantly elastic–plastic for $1.0<\psi<3.2$, and predominantly plastic for $\psi>3.2$. In the present study, values of ψ are taken as 0.7, 2.0 and 3.5, i.e. care is taken to select the values of plasticity index such that we cover all types of contact situations. Typical values of root mean square value of surface roughness (σ) for nano to micro scale surfaces are in the range of 59 nm to 0.3 μm and correlation length, $\beta^* = 6.5\ \mu m$ [28]. For metals like steel the average value of elastic modulus is 210 GPa and Poisson's ratio is 0.29. With this the reduced or equivalent modulus of elasticity works out as 114 GPa. The variation in hardness value of steel is taken in the range $0.8 - 3.9$ GPa depending on the carbon content. With these values, the plasticity index for such small scale rough surfaces comes out to be in the range of 0.7–3.5. As per Israelachivili [29], many materials have surface energies of the order 0.01–0.05 J/m^2 and metals typically have higher values of the order 0.4–4 J/m^2. The interfacial energies are of the same order of magnitude as surface energies. Thus with realistic estimate of surface roughness values and material property values as mentioned, the adhesion index(ϕ) lies in the range of 0.01–0.9. The same range of adhesion index values are used in the present study.

Apart from ϕ and ψ, the values of three other parameters, β^*(correlation length), ρ (correlation coefficient) and n_{max} (maximum number of height ordinates considered in n-point asperity) need to be fixed in order to evaluate the dimensionless loads. Physically, correlation length (β^*) gives an indication of the nature of the profile or surface. It represents the maximum distance over which significant correlation in roughness heights exist. In other words correlation length is the distance between two statistically independent points. Smoother surfaces generally have large correlation lengths while rougher surfaces have low values of correlation lengths. A profile of white noise (representing perfectly rough surface) have zero correlation length while a straight line profile (representing perfectly smooth surface) have correlation length equal to infinity. RMS height and correlation length gives roughness measure on vertical and horizontal scale respectively. Thus we can say that the roughness of surface corresponds to high values of RMS heights and low values of correlation lengths. A surface profile with low value of correlation length will carry sharp asperities while that having high value of correlation length will have flat asperities. In the present study value of correlation length (β^*) is chosen as 6.5 μm which is same as that used in earlier studies [21,22].

Correlation coefficient (ρ) defines the extent of similarity between the asperities and it carries values in between 0 and 1. For high correlation coefficient, the surface will carry highly correlated or highly similar asperities, and vice versa. The choices of ρ and n_{max} (maximum value of n or maximum value of the number of height ordinates of which an asperity is comprised of) are dependent on each other. The value of ρ dictates the choice of n_{max} to a large extent. Hariri et al. [20] have shown that for low value of ρ, lower value of n_{max} is sufficient and for high value of ρ, higher value of n_{max} is required. Earlier studies [21,22] have shown that with $\rho = 0.1$ and $n_{max} = 7$ accurate results can be obtained down to $h = 0$. In the present work also asperities with maximum up to 7 number of ordinates ($n_{max} = 7$) are considered but with $\rho = 0.5$. This selected value of correlation coefficient represents a compromise value between the maximum and minimum values of correlation. Though it is better to consider higher n_{max} for a particular value of ρ but it increases the numerical computational complexity with almost negligible improvement in accuracy. In this case, h/σ is considered between 0 and +2 and for Gaussian distribution of asperity heights this range of separation covers 95% of the asperities.

Figs. 5 and 6 show the plots of non-dimensional applied load against non-dimensional separation between contacting surfaces for different combinations of adhesion index (ϕ) and plasticity index(ψ). Fig. 5 shows the plots as function of adhesion index (ϕ) in three different zones, viz. predominantly plastic zone of contact ($\psi = 0.7$), elastic–plastic zone of contact ($\psi = 2.0$) and predominantly elastic zone of contact ($\psi = 3.5$); while Fig. 6 shows the plots as function of plasticity index (ψ) in three different zones of adhesion effect, viz. low adhesion contact ($\phi = 0.1$), moderate or medium adhesion contact ($\phi = 0.5$) and high adhesion contact ($\phi = 0.9$). Positive values of applied load indicate that compressive load needs to be applied to maintain particular level of separation between contacting surfaces while negative values of applied load indicate that tensile force needs to be applied to maintain particular level of separation. It can be seen from the plots in Fig. 5 that with increase in adhesion effect (i.e. increase in ϕ value), the tensile force required for maintaining a particular level of separation increases. Though the nature of variation of applied load with mean separation is similar; however, it may be noted that for elastic plastic contact situation ($\psi = 2.0$) and at moderate adhesion ($\phi = 0.5$), applied load is positive particularly for mean separation more than 1. Also for this parametric combination of adhesion index and plasticity index, the load-separation behavior is somewhat different from that for either low or high adhesion case. It can also be seen in the plots of Fig. 6 that as we move from predominantly elastic to predominantly plastic zone of contact, the tensile force required for maintaining a particular level of separation increases. These results clearly illustrate the relative influence of adhesion due to elastically and plastically deformed asperities on loading. The load-separation behavior is largely influenced by both adhesion and elastic plastic contact condition. The total load comprises two parts—attraction between the surfaces due to adhesion and forces arising out of the deformation of the rough surface, which tries to force the surfaces apart. In the cases considered here, the adhesion effect being stronger than the deformation forces, the total load comes out as negative, which signifies that in order to keep the surfaces apart at a certain separation tensile force from outside is to be applied at the contact.

Fig. 7 shows the plots of non-dimensional friction force against non-dimensional separation as a function of plasticity index (ψ) in three different zones of adhesion: (a) low adhesion zone of contact ($\phi = 0.1$); (b) moderate adhesion zone of contact ($\phi = 0.5$); (c) high adhesion zone of contact ($\phi = 0.9$). The behavior observed for friction or tangential load is same as that for applied load explained

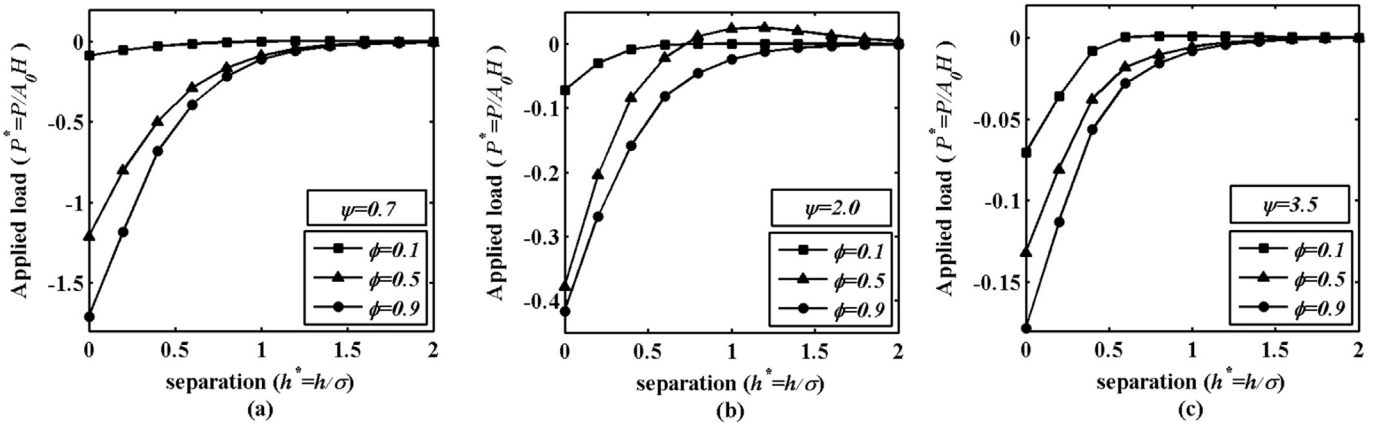

Fig. 5. Non-dimensional applied load against non-dimensional separation as function of adhesion index (ϕ) in – (a) predominantly plastic zone of contact($\psi = 0.7$); (b) elastic–plastic zone of contact($\psi = 2.0$); (c) predominantly elastic zone of contact($\psi = 3.5$).

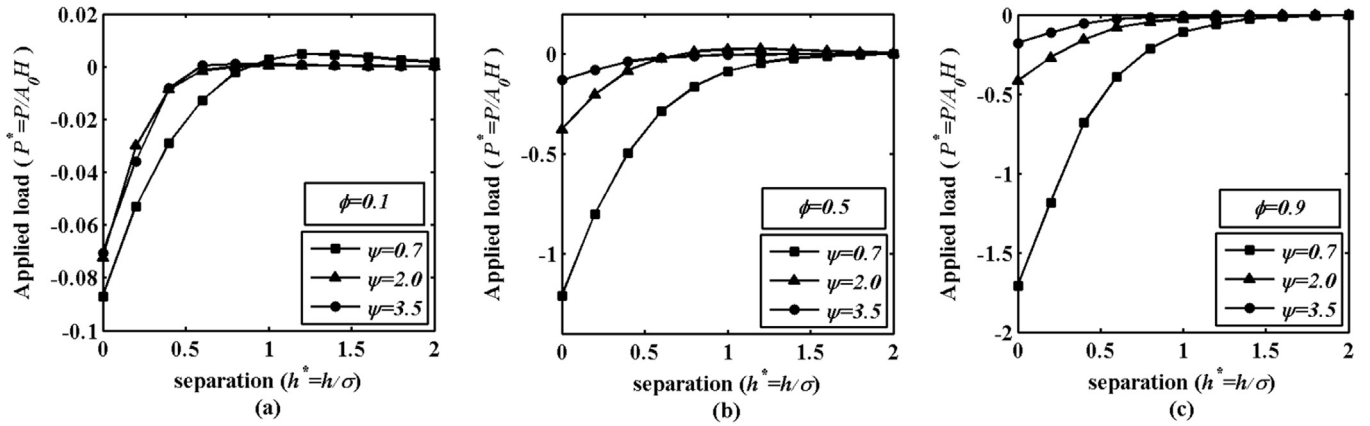

Fig. 6. Non-dimensional applied load against non-dimensional separation as function of plasticity index (ψ) in – (a) low adhesion zone of contact($\phi = 0.1$); (b) moderate adhesion zone of contact($\phi = 0.5$); (c) high adhesion zone of contact($\phi = 0.9$).

above i.e. as we move from predominantly elastic zone of contact to predominantly plastic zone of contact, the friction force at a particular level of separation increases. Fig. 8 shows non-dimensional applied load (P^*) against non-dimensional friction force (T^*) as a function of adhesion index (ϕ) in predominantly plastic zone of contact($\psi = 0.7$). It can be seen in the plot that for appreciable adhesion effect ($\phi = 0.1, 0.5$ *and* 0.9), applied load is of tensile nature (negative load values) where as for negligible adhesion effect ($\phi = 0.01$ and 0.05), applied load is of compressive nature (positive load values). Also it can be seen that in the adhesive contact zone there is direct proportionality between applied load and friction force where as with negligible adhesion this

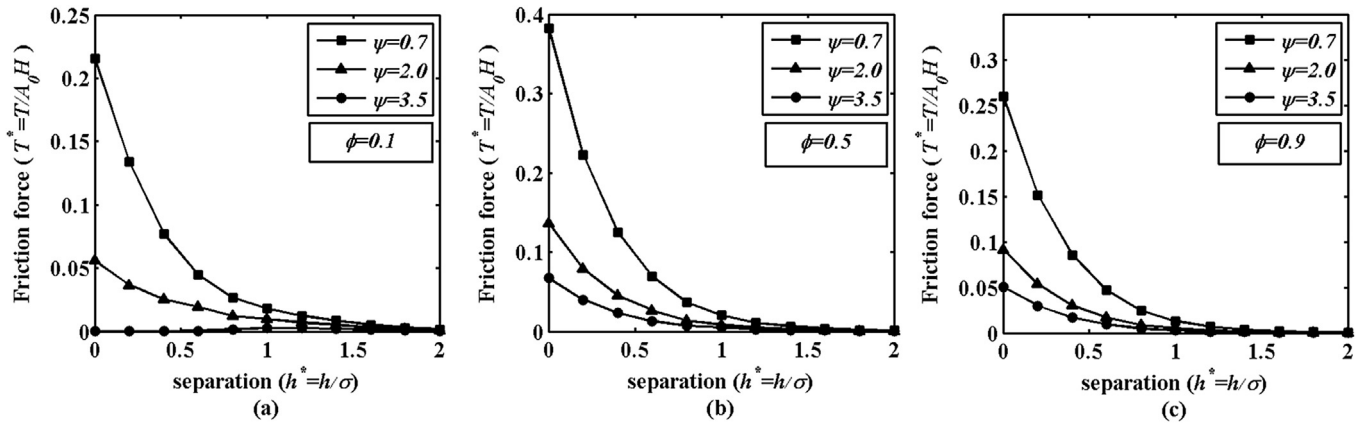

Fig. 7. Non-dimensional friction force against non-dimensional separation as function of plasticity index (ψ) in – (a) low adhesion zone of contact($\phi = 0.1$); (b) moderate adhesion zone of contact($\phi = 0.5$); (c) high adhesion zone of contact($\phi = 0.9$).

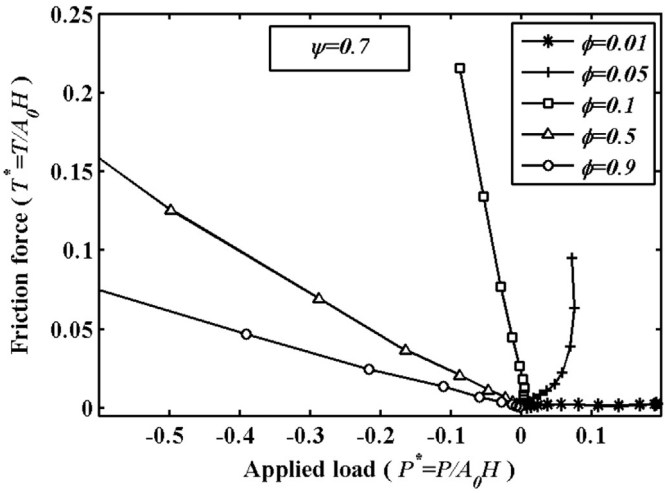

Fig. 8. Non-dimensional friction force against non-dimensional applied load as function of adhesion index (ϕ) in predominantly plastic zone of contact($\psi = 0.7$).

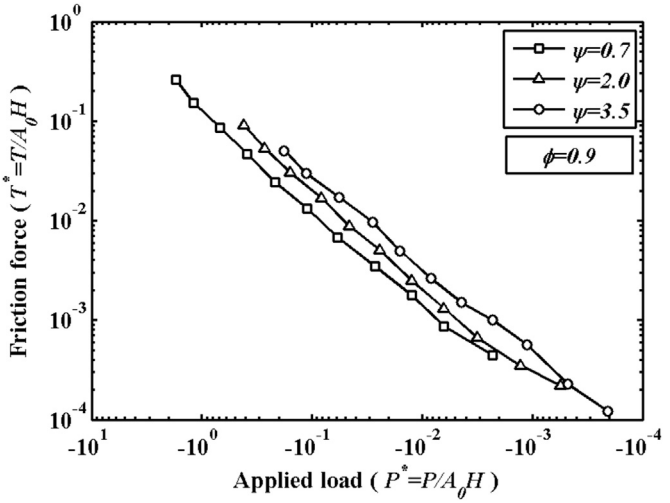

Fig. 10. Non-dimensional friction force against non-dimensional applied load as function of plasticity index (ψ) in high adhesion zone of contact($\phi = 0.9$) on log–log scale.

proportionality vanishes. This implies that the frictional effect is proportional to adhesion effect. This trend of behavior observed in the present study is same as that found in Roy Chowdhury and Ghosh [8] analysis.

Fig. 9 shows non-dimensional applied load (P^*) against non-dimensional friction force (T^*) as a function of plasticity index (ψ) in predominantly high adhesive zone of contact($\phi = 0.9$). It can be seen that for the same applied load, friction force is more in predominantly elastic type of contact than the predominantly plastic type of contact. This behavior implies that higher the plastic deformation of contacting asperities, lesser will be the tangential resistance offered by the surface. This is in line with the consideration of the present analysis that plastically deformed asperities offer negligible resistance. This trend of behavior observed in the present study is qualitatively same as that found in Kogut and Etsion [16] static friction model. Fig. 10 shows a plot on log–log scale for non-dimensional applied load (P^*) against non-dimensional friction force (T^*) as a function of plasticity index (ψ) in predominantly adhesive zone of contact($\phi = 0.9$). It can be seen from the plot that for the same applied load, friction force is more in predominantly elastic type of contact than the predominantly plastic type of contact. As in earlier plot this trend of behavior again implies that higher plastic deformation of contacting asperities yields lesser tangential resistance offered by the surface. Fig. 11 shows a plot on semi-log scale for non-dimensional applied load (P^*) against coefficient of friction as a function of plasticity index(ψ) in predominantly adhesive zone of contact($\phi = 0.9$). It can be seen that the coefficient of friction is in general higher for predominantly elastic deformation of surfaces and vice versa. As the plasticity index (ψ) tends to zero, the deformation tends to fully plastic and thus the coefficient of friction also tends to zero. This trend can be clearly observed in Fig. 11.

From the present results it is possible to locate the combinations of adhesion index and plasticity index that may yield very low coefficient friction. Thus suitable choice of surface and material parameters for the contact of two rough surfaces can be made in order to minimize friction typically at low load and micro scale

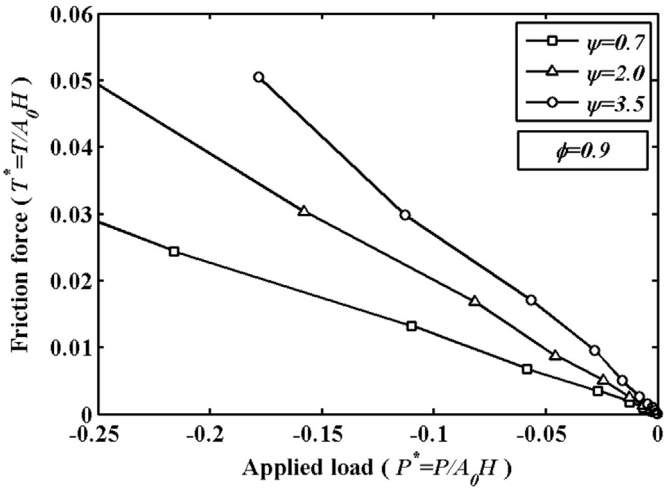

Fig. 9. Non-dimensional friction force against non-dimensional applied load as function of plasticity index (ψ) in high adhesion zone of contact($\phi = 0.9$).

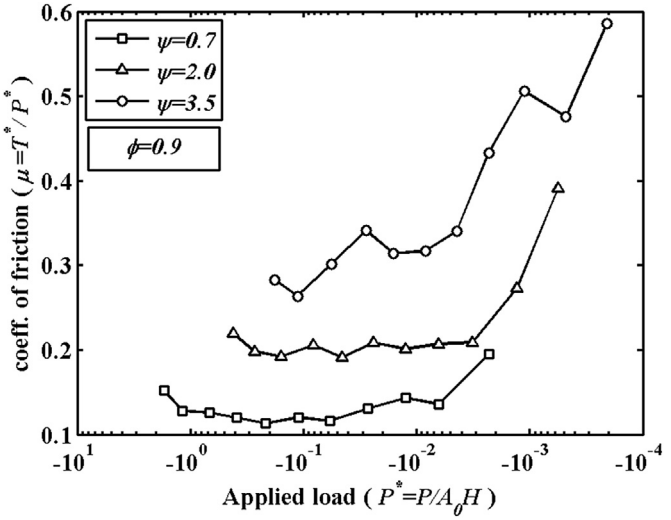

Fig. 11. Coefficient of friction against non-dimensional applied load as function of plasticity index (ψ) in high adhesion zone of contact($\phi = 0.9$) on semi-log scale.

roughness situations. It may be mentioned here that direct comparison of the present results with other adhesive friction models like Kogut and Etsion [16] that uses conventional three point asperity considerations would have been very useful. In order to compare the two models, a suitable constant value for the radius of asperity tip is required to establish equivalence and finding such a value for the parameter is quite difficult. As can be seen from the expression of equivalent asperity radius, the value would also depend on the sampling length and the conventional models do not consider the sampling length at all. Thus, a comparison with such earlier model [16] could not be made. Moreover, the present study considers only the JKR model, one extreme of adhesive contact which is valid for soft solids with large surface energy and radius. However, future work may consider the DMT model, the other extreme of adhesive contact which is applicable to hard solids of small radius and low surface energy. It may also be noted that the present analysis has been considered for linearly elastic–plastic materials. But for other materials like viscoelastic ones having micro and macro hysteresis characteristics, the present procedure is not straightway applicable as the present analysis is based on the plasticity consideration at the asperity level contact. Adoption of the present procedure for viscoelastic materials will require separate considerations that may define a scope for future study.

5. Conclusions

The n-point asperity model takes into account the change of the asperity with progression of contact. Hence, it represents a more realistic situation than the conventional three-point asperity models. The present analysis considers adhesive friction between rough surfaces for JKR contacts using the n-point asperity model. The friction behavior of contacting surfaces is conveniently described in terms of a newly defined adhesion index and a plasticity index defined for the n-point asperity model. It is clearly seen that the tensile load required in maintaining a separation increases with increase in adhesion effect and plastic deformation. Also friction behavior is proportional to adhesion effect and coefficient of friction is in general higher for predominantly elastic deformation of surfaces. Surface and material parameters for the contact of two micro scale rough surfaces can be chosen suitably in order to control friction at adhesion dominated contact situations.

Notations

A_0	total nominal contact area of rough surface (sample space)
$a_{(e)_n}$	contact radius of an n-point asperity in elastic mode of deformation
$a_{(p)_n}$	contact radius of an n-point asperity in plastic mode of deformation
c_n	curvature coefficient
$c_{(1)_n}$	critical curvature coefficient marking transition from elastic to plastic state
C_n	curvature of an equivalent n-point asperity, $C_n = c_n\sigma$
E	composite elastic modulus of an equivalent rough surface$E = [(1-\upsilon_1^2)/E_1 + (1-\upsilon_2^2)/E_2]^{-1}$
E_1,E_2	elastic modulus for two surfaces in contact
$f(z)$	joint probability density functions for height ordinates
H	hardness of soft surface
h	separation between mean surface line of equivalent rough surface and rigid smooth surface
K	elastic constant, $K = 4/3E$
M	number of sampled points
M_n	total number of n-point asperities having specific 'n' value
$M_{(e)_n}$	total number of n-point asperities supporting elastic load and having specific 'n' value
$M_{(p)_n}$	total number of n-point asperities supporting plastic load and having specific 'n' value
n	number of height ordinates defining an n-point asperity
N_n	probability of existence above a defined level for n-point asperities having specific 'n' value
$N_{(e)_n}$	probability of existence above a defined level for n-point asperities having specific 'n' value and undergoing elastic deformation only
$N_{(p)_n}$	probability of existence above a defined level for n-point asperities having specific 'n' value and undergoing plastic deformation only
P	total applied load on an equivalent rough surface
P^*	non dimensional total applied load, $P^*=P/A_0H$
P_S	total force due to adhesion surface energy on an equivalent rough surface
P_n	total applied load supported by all n-point asperities having specific 'n' value
P_n^*	non dimensional total applied load supported by all n-point asperities having specific 'n' value
$\Delta P_{(e)_n}$	load supported by single n-point asperity having specific 'n' value in elastic domain
$\Delta P_{(p)_n}$	load supported by single n-point asperity having specific 'n' value in plastic domain
$P_{(e)_n}$	load supported by all n-point asperities having specific 'n' value in elastic domain
$P_{(p)_n}$	load supported by all n-point asperities having specific 'n' value in plastic domain
R_n	radius of equivalent n-point asperity curve
T	total tangential or friction force on equivalent rough surface
T^*	non dimensional total tangential or friction force, $T^*=T/(A_0H)$
T_n^*	non dimensional total tangential or friction force supported by all n-point asperities having specific 'n' value
$T^*_{(slip)_n}$	non dimensional total tangential or friction force supported by all n-point asperities having specific 'n' value before slip
$T^*_{(yield)_n}$	non dimensional total tangential or friction force supported by all n-point asperities having specific 'n' value before yield
$\Delta T^*_{(slip)_n}$	non dimensional tangential or friction force supported by single n-point asperity having specific 'n' value before slip
$\Delta T^*_{(yield)_n}$	non dimensional tangential or friction force supported by single n-point asperity having specific 'n' value before yield
Δx	sampling length, $\Delta x=\beta^*(-In\rho)$
z_n	height of nth ordinate from mean surface line
z_n^*	$=z_n/\sigma$
z_0	height of equivalent n-point asperity curve
z_0^*	$=z_0/\sigma$
β^*	correlation length
γ	work of adhesion
δ_n	real interference of an n-point asperity having specific 'n' value
$\delta_{(0)_n}$	apparent zero interference of an n-point asperity having specific 'n' value
$\delta_{(1)_n}$	apparent interference of an n-point asperity having specific 'n' value
$\delta_{(c)_n}$	real critical interference of an n-point asperity having specific 'n' value
$\delta_{(c_1)_n}$	apparent critical interference of an n-point asperity having specific 'n' value

$\delta_{(tc_1)_n}$ apparent critical interference in tangential loading on an n-point asperity having specific 'n' value
δ_n^* $=\delta_n/\sigma$; non dimensional real interference of an n-point having specific 'n' value
ϕ $=\gamma\beta^*/E\sigma^2$; adhesion index
ψ $=H\beta^*/E\sigma$; plasticity index
ρ correlation coefficient
σ root mean square roughness or standard deviation of height ordinates
μ $=T^*/P^*$; coefficient of friction
υ Poisson's ratio
ξ $=(n-2)z_0^*-(n-4)c/6$

Appendix

A.1. Calculation for elastic load in adhesive contact

Calculations for applied load for adhesive elastic contact for all the asperities having specific n value and which is as given in equation (14) are carried out as given below

$$P^*_{(e)_n}=M_{(e)_n}E\left[\Delta P^*_{(e)_n}\right] \quad \text{for } \delta^*_{(0)_n}\le\delta^*_n\le\delta^*_{(c_1)_n}$$

$$M_{(e)_n}=M\times N_{(e)_n}$$

where $N_{(e)_n}$ is the probability of existence of an elastically deformed n-point asperity in the deformation zone $\delta^*_{(0)_n}\le\delta^*_n\le\delta^*_{(c_1)_n}$ and is evaluated from eq. (1) by modifying limits of integrations accordingly.
for $n=3,4$

$$P^*_{(e)_n}=\left(\frac{2(n-1)}{\psi(-\ln\rho)}\right)\int_{c_n=0}^{c(1)_n}\int_{z_0^*=h^*+\delta^*_{(0)_n}}^{h^*+c_n/2}\int_{z_1^*=2z_0-h^*-c_n}^{h^*}\int_{z^*_{n-2}=h^*}^{2z_0^*-h^*}\times\left[\frac{2\left(z_0^*-h^*\right)^{3/2}}{3c_n^{1/2}}-\frac{1.77(n-1)^{1/2}(-\ln\rho)^{1/2}\left(z_0^*-h^*\right)^{3/4}}{c_n^{3/4}}\phi^{1/2}\right]$$
$$\times\frac{e^{-z_1^{*2}/2}}{(2\pi)^{n/2}\left(1-\rho^2\right)^{(n-1)/2}}\prod_{i=n-1}^{1}e^{-\left[\left(z^*_{i+1}-\rho z_i^*\right)^2/2(1-\rho^2)\right]}dz^*_{n-2}d^*_{z_1}d^*_{z_0}dc_n \tag{28}$$

for $n>4$

$$P^*_{(e)_n}=\left(\frac{2(n-1)^2}{3\psi(-\ln\rho)}\right)\left(\int_{c_n=0}^{c_{(1)n}}\int_{z_0^*=h^*+\delta^*_{(0)_n}}^{h^*+c_n/2}+\int_{c_n=c_{(1)n}}^{c_{(2)n}}\int_{z_0^*=h^*+\delta^*_{(0)_n}+\frac{(n-4)c_n}{6(n-2)}}^{h^*+\delta^*_{(c_1)_n}}\cdots\right)\times\int_{z_1^*=2z_0^*-h^*-c_n}^{h^*}\int_{z^*_{n-2}=h^*}^{\xi-(n-3)h^*}\cdots$$
$$\times\int_{z_i^*=h^*}^{\xi-(i-1)h^*-\sum_{j=i+1}^{n-2}z_j^*}\int_{z_2^*=h^*}^{\xi-h^*-\sum_{j=3}^{n-2}z_j^*}\times\left[\frac{2\left(z_0^*-h^*\right)^{3/2}}{3c_n^{1/2}}-\frac{1.77(n-1)^{1/2}(-\ln\rho)^{1/2}\left(z_0^*-h^*\right)^{3/4}}{c_n^{3/4}}\phi^{1/2}\right]$$
$$\times\frac{e^{-z_1^{*2}/2}}{(2\pi)^{n/2}\left(1-\rho^2\right)^{(n-1)/2}}\prod_{i=n-1}^{1}e^{-\left[\left(z^*_{i+1}-\rho z_i^*\right)^2/2(1-\rho^2)\right]}dz_2^*\ldots dz^*_{n-2}d^*_{z_1}d^*_{z_0}dc_n \tag{29}$$

A.2. Calculation for plastic load in adhesive contact

Calculations for applied load for adhesive plastic contact for all the asperities having specific n value and which is as given in equation (15) are carried out as given below

$$P^*_{(p)_n}=M_{(p)_n}E\left[\Delta P^*_{(p)_n}\right] \quad \text{for } \delta^*_{(c)_n}\le\delta^*_n\le\infty$$

$$M_{(p)_n}=M\times N_{(p)_n}$$

where $N_{(p)_n}$ is the probability of existence of a plastically deformed n-point asperity in the deformation zone $\delta^*_{(c)_n}\le\delta^*_n\le\infty$.for $n=3,4$

$$P^*_{(p)_n}=\pi(n-1)^2\int_{c_n=c_{(1)n}}^{\infty}\int_{z_0^*=h^*+\delta^*_{(c)n}}^{h^*+c_n/2}\int_{z_1^*=2z_0^*-h^*-c_n}^{h^*}\int_{z^*_{n-2}=h^*}^{2z_0^*-h^*}\times\left[\frac{\left(z_0^*-h^*\right)}{c_n}-\frac{\phi}{c_n\psi}\right]\times\frac{e^{-z_1^{*2}/2}}{(2\pi)^{n/2}\left(1-\rho^2\right)^{(n-1)/2}}$$
$$\times\prod_{i=n-1}^{1}e^{-\left[\left(z^*_{i+1}-\rho z_i^*\right)^2/2(1-\rho^2)\right]}dz^*_{n-2}d^*_{z_1}d^*_{z_0}dc_n \tag{30}$$

for $n>4$

$$P^*_{(p)_n} = \frac{\pi(n-1)^3}{3} \times \left(\int_{c_n=c_{(1)_n}}^{c_{(2)_n}} \int_{z_0^*=h^*+\delta^*_{(c)_n}}^{h^*+c_n/2} + \int_{c_n=c_{(2)_n}}^{\infty} \int_{z_0^*=h^*+\delta^*_{(c)_n}+\frac{(n-4)c_n}{6(n-2)}}^{h^*+c_n/2} \cdots \right) \times \int_{z_1^*=2z_0^*-h^*-c_n}^{h^*} \int_{z_{n-2}^*=h^*}^{\xi-(n-3)h^*} \cdots$$

$$\times \int_{z_i^*=h^*}^{\xi-(i-1)h^*-\sum_{j=i+1}^{n-2} z_j^*} \int_{z_2^*=h^*}^{\xi-h^*-\sum_{j=3}^{n-2} z_j^*} \left[\frac{\left(z_0^*-h^*\right)}{c_n} - \frac{\phi}{c_n\psi} \right] \times \frac{e^{-z_1^{*2}/2}}{(2\pi)^{n/2}\left(1-\rho^2\right)^{(n-1)/2}} \prod_{i=n-1}^{1} e^{-\left[\left(z_{i+1}^*-\rho z_i^*\right)^2/2\left(1-\rho^2\right)\right]} dz_2^* \ldots dz_{n-2}^* d_{z_1}^* d_{z_0}^* dc_n \tag{31}$$

A.3. Tangential load for slipping

Calculations for tangential slip load for all the asperities having specific n value and which is as given in equation (20) are carried out as given below

$$T^*_{(slip)_n} = M_{(slip)_n} E\left[\Delta T^*_{(slip)_n}\right] \quad \text{for interference range } \delta^*_{(0)_n} \le \delta_n^* \le \delta^*_{(tc_1)_n}$$

$$M_{(slip)_n} = M \times N_{(slip)_n}$$

for $n = 3,4$

$$T^*_{(slip)_n} = 5 \times \left(\frac{1-\nu}{2-\nu}\right)^{\frac{1}{2}} \int_{c_n=0}^{c_{(t_1)_n}} \int_{z_0^*=h^*+\delta^*_{(0)_n}}^{h^*+\delta^*_{(tc_1)_n}} \int_{z_1^*=2z_0^*-h^*-c_n}^{h^*} \int_{z_{n-2}^*=h^*}^{2z_0^*-h^*} \times \left\{ \frac{(n-1)^3\left(z_0^*-h^*\right)^{3/2}}{(-\ln\rho)c_n^{3/2}} \frac{\phi}{\psi^2} - 1.77\frac{(n-1)^4}{c_n^2}\frac{\phi^2}{\psi^2} \right\}^{\frac{1}{2}}$$

$$\times \frac{e^{-z_1^{*2}/2}}{(2\pi)^{n/2}\left(1-\rho^2\right)^{(n-1)/2}} \prod_{i=n-1}^{1} e^{-\left[\left(z_{i+1}^*-\rho z_i^*\right)^2/2\left(1-\rho^2\right)\right]} dz_{n-2}^* d_{z_1}^* d_{z_0}^* dc_n \tag{32}$$

for $n>4$

$$T^*_{(slip)_n} = 1.67 \times \left(\frac{1-\nu}{2-\nu}\right)^{\frac{1}{2}} \times \left(\int_{c_n=0}^{c_{(t_1)_n}} \int_{z_0^*=h^*+\delta^*_{(0)_n}}^{h^*+\delta^*_{(tc_1)_n}} + \int_{c_n=c_{(t_1)_n}}^{c_{(t_2)_n}} \int_{z_0^*=h^*+\delta^*_{(0)_n}+\frac{(n-4)c_n}{6(n-2)}}^{h^*+\delta^*_{(tc_1)_n}} \cdots \right) \times \int_{z_1^*=2z_0^*-h^*-c_n}^{h^*} \int_{z_{n-2}^*=h^*}^{\xi-(n-3)h^*} \cdots$$

$$\times \int_{z_i^*=h^*}^{\xi-(i-1)h^*-\sum_{j=i+1}^{n-2} z_j^*} \int_{z_2^*=h^*}^{\xi-h^*-\sum_{j=3}^{n-2} z_j^*} \times \left\{ \frac{(n-1)^5\left(z_0^*-h^*\right)^{3/2}}{(-\ln\rho)c_n^{3/2}} \frac{\phi}{\psi^2} - 1.77\frac{(n-1)^6}{c_n^2}\frac{\phi^2}{\psi^2} \right\}^{\frac{1}{2}}$$

$$\times \frac{e^{-z_1^{*2}/2}}{(2\pi)^{n/2}\left(1-\rho^2\right)^{(n-1)/2}} \prod_{i=n-1}^{1} e^{-\left[\left(z_{i+1}^*-\rho z_i^*\right)^2/2\left(1-\rho^2\right)\right]} dz_2^* \ldots dz_{n-2}^* d_{z_1}^* d_{z_0}^* dc_n \tag{33}$$

A.4. Tangential load for yielding

Calculations for tangential yield load for all the asperities having specific n value and which is as given in equation (22) are carried out as given below

$$T^*_{(yield)_n} = M_{(yield)_n} E\left[\Delta T^*_{(yield)_n}\right] \quad \text{for } \delta^*_{(tc_1)_n} \le \delta_n^* \le \delta^*_{(c_1)_n}$$

$$M_{(yield)_n} = M \times N_{(yield)_n}$$

for $n = 3,4$

$$T^*_{(yield)_n} = 2 \times M \times \int_{c_n=c_{(t_1)_n}}^{c_{(1)n}} \int_{z_0^*=h^*+\delta^*_{(tc_1)_n}}^{h^*+\delta^*_{(c_1)_n}} \int_{z_1^*=2z_0^*-h^*-c_n}^{h^*} \int_{z_{n-2}^*=h^*}^{2z_0^*-h^*} \left(\Delta T^*_{(yield)_n}\right) \times \frac{e^{-z_1^{*2}/2}}{(2\pi)^{n/2}\left(1-\rho^2\right)^{(n-1)/2}} \prod_{i=n-1}^{1} e^{-\left[\left(z^*_{i+1}-\rho z_i^*\right)^2/2\left(1-\rho^2\right)\right]} dz^*_{n-2} d^*_{z_1} d^*_{z_0} dc_n \tag{34}$$

for $n>4$

$$T^*_{(yield)_n} = \frac{2(n-1)}{3} \times M \times \left(\int_{c_n=c_{(t_1)_n}}^{c_{(1)n}} \int_{z_0^*=h^*+\delta^*_{(tc_1)_n}}^{h^*+\delta^*_{(c_1)_n}} + \int_{c_n=c_{(1)n}}^{c_{(2)n}} \int_{z_0^*=h^*+\delta^*_{(tc_1)_n}+\frac{(n-4)c_n}{6(n-2)}}^{h^*+\delta^*_{(c_1)_n}} \cdots \right) \times \int_{z_1^*=2z_0^*-h^*-c_n}^{h^*} \int_{z_{n-2}^*=h^*}^{\xi-(n-3)h^*} \cdots$$
$$\times \int_{z_i^*=h^*}^{\xi-(i-1)h^*-\sum_{j=i+1}^{n-2} z_j^*} \int_{z_2^*=h^*}^{\xi-h^*-\sum_{j=3}^{n-2} z_j^*} \times \left(\Delta T^*_{(yield)_n}\right) \times \frac{e^{-z_1^{*2}/2}}{(2\pi)^{n/2}\left(1-\rho^2\right)^{(n-1)/2}} \times \prod_{i=n-1}^{1} e^{-\left[\left(z^*_{i+1}-\rho z_i^*\right)^2/2\left(1-\rho^2\right)\right]} dz_2^* \ldots dz^*_{n-2} d^*_{z_1} d^*_{z_0} dc_n \tag{35}$$

References

[1] F.P. Bowden, D. Tabor, The Friction and Lubrication of Solids, Clarendon Press, Oxford, 1954.
[2] J. Skinner, N. Gane, Sliding friction under a negative load, J. Phys. D: Appl. Phys. 5 (1972) 2087–2094.
[3] A.R. Savkoor, G.A.D. Briggs, The effect of tangential force on the contact of elastic solids in adhesion, Proc. Royal Soc. Lond. Ser. A 356 (1977) 103–114.
[4] K.L. Johnson, Friction and traction, in: D. Dowson, C.M. Taylor, M. Godet, D. Berthe (Eds.), Westbury House, IPC Press, Guildford, United Kingdom, 1981, p. 3.
[5] H.M. Pollock, Surface forces and adhesion. In fundamentals of friction, in: I.L. Singer, H.M. Pollock (Eds.), Macroscopic and Microscopic Prcesses, Kluwer Academic Publishers, London, 1992, pp. 77–94.
[6] I. Etsion, M. Amit, The effect of small normal loads on the static friction coefficient for very smooth surfaces, Trans. ASME J. Tribol. 115 (1993) 406–410.
[7] J. Israelachvili, Y.L. Chen, H. Yoshizawa, Relationship between adhesion and friction forces, J. Adhesion Sci. Techno. 8 (1994) 1–18.
[8] S.K. Roy Chowdhury, P. Ghosh, Adhesion and adhesional friction at the contact between solids, Wear 174 (1994) 9–19.
[9] K.L. Johnson, K. Kendall, A.D. Roberts, Surface energy and the contact of elastic solids, Proc. Royal Soc. Lond. Ser. A 324 (1971) 301–313.
[10] B.V. Derjaguin, V.M. Muller, Y.P. Toporov, Effect of contact deformation on adhesion of elastic solids, J. Colloid Interface Sciences 53 (1975) 314–326.
[11] D. Maugis, On the contact and adhesion of rough surfaces, J. Adhesion Sci. Techno. 10 (1996) 161–175.
[12] K.L. Johnson, Adhesion and friction between a smooth elastic spherical asperity and a plane surface, Proc. Royal Soc. Lond. Ser. A 453 (1997) 163–179.
[13] P. Sahoo, S.K. Roy Chowdhury, A fractal analysis of adhesive friction between rough solids in gentle sliding, Proc. Inst. Mech. Eng. 214 (2000) 583–595.
[14] S.M. Ali, P. Sahoo, Adhesive friction for elastic-plastic contacting rough surfaces using a scale dependent model, J. Phy. D: Appl. Phys. 39 (2006) 721–729.
[15] P. Sahoo, Adhesive friction for elastic-plastic contacting rough surfaces considering asperity interaction, J. Phys. D: Appl. Phys. 39 (2006) 2809–2818.
[16] L. Kogut, I. Etsion, A static friction model for elastic-plastic contacting rough surfaces, Trans. ASME J. Tribol. 126 (2004) 34–40.
[17] J.A. Greenwood, J.B.P. Williamson, Contact of nominally flat surfaces, Proc. Royal Soc. Lon. Ser. A 295 (1966) 300–319.
[18] J.A. Greenwood, J.J. Wu, Surface roughness and contact: an apology, Meccanica 36 (6) (2001) 617–630.
[19] J.F. Archard, Elastic deformation and the laws of friction, Proc. Royal Soc. Lond. Ser. A 243 (1957) 190–205.
[20] A. Hariri, J.W. Zu, R. Ben Mrad, n-Point asperity model for contact between nominally flat surfaces, ASME J. Tribol. 128 (2006) 505–514.
[21] A. Hariri, J.W. Zu, R. Ben Mrad, Modeling of Elastic/Plastic contact between nominally flat rough surfaces using an n-Point asperity model, ASME J. Tribol. 128 (2006) 876–885.
[22] P. Sahoo, A. Mitra, K. Saha, Elastic-plastic adhesive contact of rough surfaces using n-Point asperity model, J. Phys. D: Appl. Phys. 42 (2009) 1–13.
[23] S.K. Roy Chowdhury, H.M. Pollock, Adhesion between metal surfaces: the effect of surface roughness, Wear 66 (1981) 307–321.
[24] J.A. Greenwood, J.H. Tripp, The contact of two nominally flat rough surfaces, Proc. Ins.Mech. Eng. 185 (1971) 625–633.
[25] M. O'Callaghan, M.A. Cameron, Static contact under load between nominally flat surfaces in which deformation is purely elastic, Wear 36 (1976) 79–97.
[26] G.M. Hamilton, Explicit equations for the stresses beneath a sliding spherical contact, Proc. Ins. Mech. Eng. 197 (C) (1983) 53–59.
[27] K.L. Johnson, Adhesion at the contact of solids, in: W.T. Koiter (Ed.), 4th IUTAM Congress Proceedings on Theoretical and Applied Mechanics, 1976, pp. 133–143. Amsterdam: North-Holland.
[28] D.J. Whitehouse, J.F. Archard, The properties of random surfaces of significance in their contact, Proc. Royal Soc. Lond. A. Math. Phys. Sci. 316 (1524) (1970) 97–121.
[29] J.N. Israelachvili, Intermolecular and Surface Forces, revised third ed., Academic Press, 2011, p. 280.